2017 IEEE/RSJ International Conference on Intelligent Robots and Systems (IROS)
September 24–28, 2017, Vancouver, BC, Canada

# Real-Time End-Effector Motion Behavior Planning Approach Using On-line Point-Cloud Data Towards a User Adaptive Assistive Bath Robot

Athanasios C. Dometios, Xanthi S. Papageorgiou, Antonis Arvanitakis, Costas S. Tzafestas, and Petros Maragos
School of Electrical and Computer Engineering, National Technical University of Athens, Greece
{athdom,xpapag}@mail.ntua.gr, {ktzaf,maragos}@cs.ntua.gr

***Abstract*— Elderly people have particular needs in performing bathing activities, since these tasks require body flexibility. Our aim is to build an assistive robotic bath system, in order to increase the independence and safety of this procedure. Towards this end, the expertise of professional carers for bathing sequences and appropriate motions has to be adopted, in order to achieve natural, physical human - robot interaction. In this paper, a real-time end-effector motion planning method for an assistive bath robot, using on-line Point-Cloud information, is proposed. The visual feedback obtained from Kinect depth sensor is employed to adapt suitable washing paths to the user's body part motion and deformable surface. We make use of a navigation function-based controller, with guarantied globally uniformly asymptotic stability, and bijective transformations for the adaptation of the paths. Experiments were conducted with a rigid rectangular object for validation purposes, while a female subject took part to the experiment in order to evaluate and demonstrate the basic concepts of the proposed methodology.**

## I. INTRODUCTION

The results of the advances in medicine and nursing services is the increase of life expectancy and constant growth of the elderly population. Elderly people, who have special and augmented needs for nursing attention (in-house and clinical), especially in performing Personal Care Activities such as showering, dressing and eating [1], [2], will induce great financial burden both to the families and the insurance systems.

Body care (showering or bathing) is among the first daily life activities which incommode an elderly's life [1], since it is a demanding procedure in terms of effort and body flexibility. Roboticists have already proposed solutions to this basic personal care disability, with either static physical interaction [3], or mobile solutions [4]. Most of these focus exclusively on a body part e.g. the head, and support people on performing other personal care activities with rigid manipulators.

Soft robotic arm technologies have already presented new ways of thinking robot operation [5]. Autonomous continuum robot interaction with rigid and static objects in unknown working scenes, for manipulation and grasping scenarios, has been addressed in [6], [7]. However, applications with physical contact with human (such as showering) are way more demanding, since we have to deal with curved and deformable human body parts. Furthermore, unexpected body-part motion may occur during the robot's operation, therefore safety and comfort issues the washing process should be taken into account. Moreover, control architectures of a hyper-redundant soft arms [8], [9], in an environment with human motion is a challenging task, since several control aspects should be considered such as position, motion and path planning [10], stiffness [11], shape [12] control.

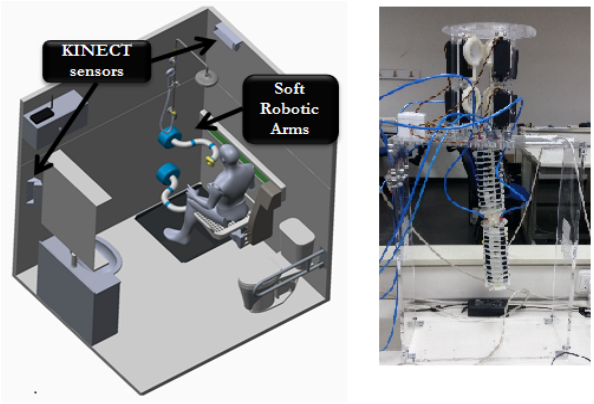


Fig. 1: CAD design of the robotic bath system installed in a pilot study shower room. The real soft-arm, which is currently under construction, is also depicted (courtesy of Sant'Anna School of Advanced Studies).

In [13], [14] a potential field based real time path planning for a tendon driven continuum style manipulator is proposed, although the aforementioned method suffers from local minima problem and therefore this algorithm does not ensure global convergence. However, solutions regarding real-time motion planning problems in static or dynamic environments towards Human Robot Interaction (HRI) were proposed in several works [15], [16].

From the perception point of view, the use of vision sensors for object detection and pose estimation in robotic applications has been investigated within the last decades. More recently, researchers have been developing algorithms

This research work has received funding from the European Union's Horizon 2020 research and innovation programme under the project "I-SUPPORT" with grant agreement No 643666 (http://www.i-support-project.eu/).

and systems, which use depth and RGB images to segment human limbs [17].

In this paper, we propose a real-time motion behavior planning approach, which exploits the visual information from Depth sensors and the advantages of a Navigation Function approach [16], in order to calculate each time-step the 6D reference pose (position and orientation) for the end-effector of a robotic manipulator. The proposed method is independent of the robot model, therefore it can be applied to any robotic manipulator. This system will help elderly during bathing, by enhancing mobility, manipulation and force exertion abilities, and increasing in that way the independence and safety of the showering activity. This is a demanding task, since suitable washing actions should be adapted on different user body-part's deformable surface and motion.

This is achieved by establishing bijective transformations between a 2D "Canonical" space (on which predefined washing paths are described) and the 3D robot's operational subspace visible by the camera, using as an intermediate the 2D Image space provided by the Depth sensors. The proposed methods are validated through real experiments by using a Kinect camera and a rigid rectangular object. This experimental setup is suitable for the evaluation and demonstration of the basic concepts of this approach. Finally, a female subject was employed, in order to demonstrate the adaptability of the proposed approach on different user size and needs.

## II. SYSTEM DESCRIPTION

The robotic shower system, which is currently under development Fig. 1, will support elderly and people with mobility disabilities during showering activities, i.e. pouring water, body part scrubbing, etc. The degree of automation will vary according to the user's preferences and disability level. In Fig. 1, a CAD design of the system's basic parts is presented.

The robotic arms will be constructed with soft materials (rubber, silicon etc.) and will be actuated with the aid of tendons and pneumatic chambers, providing the required motion to the three sections of the robotic arm, as described in [18]. This configuration makes the arms safer and more friendly for the user, since it generates little resistance to compressive forces. Moreover, the combination of these actuation techniques increases the dexterity of the soft arms and allows for adjustable stiffness in each section of the robot. The end-effector section, which will interact physically with the user, will exhibit low stiffness achieving smoother contact, while the base sections supporting the robotic structure will exhibit higher stiffness values.

Visual information of the user will be obtained from Kinect depth cameras. These cameras will be mounted on the wall of the shower room in a proper configuration, Fig. 1. It is important to mention that information exclusively from depth measurements will be used to protect the user's personal information. Accurate interpretation of the visual information is a prerequisite for human perception algorithms (e.g. accurate body part recognition and segmentation [17]) and human-system interaction [19]. Depth information will also be used as a feedback for robot control algorithms closing the loop and defining the operational space of the robotic devices.

## III. PROBLEM STATEMENT

The motion behavior problem of a robotic manipulator's end-effector, which operates over a curved deformable surface (e.g. user's body part), in a workspace equipped with a depth-camera, is considered. We assume that we have a robot which can be kinematically described by $\dot{\mathbf{q}} = \mathbf{u}$, where $\mathbf{q}$ is the vector of end-effector position and orientation, and $\mathbf{u}$ is the vector of velocity inputs. Let the admissible and feasible state space (workspace) for the robot be denoted $\mathscr{W} \subset \mathbb{R}^6$. The obstacle free subset of the workspace is denoted $\mathscr{W}_{free} \subseteq \mathscr{W}$. Let $\mathscr{O} \in \mathscr{W} \setminus \mathscr{W}_{free}$ be the set of all obstacles in 3-D workspace. These obstacles should be visible by a depth camera, whose field of view should include the workspace of the robot. Obstacle areas may regard restricted areas, either on the user's body (e.g. local injury), which should be avoided during the washing sequence, or on other body parts that interfere to the robot's motion (e.g. the hands of the user).

The core of this motion behavior task is to calculate on the fly the reference pose for the end-effector of the robotic arm, which will let the robotic manipulator execute predefined surface tasks (e.g. scrubbing the user's back) and at the same time to be compliant with this body part. This is a challenging task, since all human's body parts are non-planar surfaces, that are moving and deforming either systematically (e.g. user's breathing motion) or randomly.

Adaptability to different users is also a very important feature of the system. Different users have dissimilar body areas and needs during the washing sequence. Hence, the basic course of this paper commences with the planning of the end-effector path on a fixed 2D normalized space ("Canonical" space) as depicted in Fig. 2 (a), in order to compensate the operational variability.

In addition, proper and human friendly washing motions for each subtask should be learned by demonstration of health care experts [20]. This demonstration might raise some requirements for each task, in terms of execution time and motion complexity. These requirements can be met using ideas and algorithms from Dynamic Motion Primitives (**DMP**) approach [21].

These motions can be followed with use of the controller presented in Section IV, satisfying both the time and the spacial constraints of the motion. The resulting point from the controller should be transformed from the fixed 2D "Canonical" space to the 3D actual operational space of the robot (Task space). This is achieved with two bijective transformations, Fig. 2(b),(c), described in Section V. These bijections ensure that the path will be followed within the body part limits, will be adaptable to the body motions and deformations, and can also provide feedback to the controller.

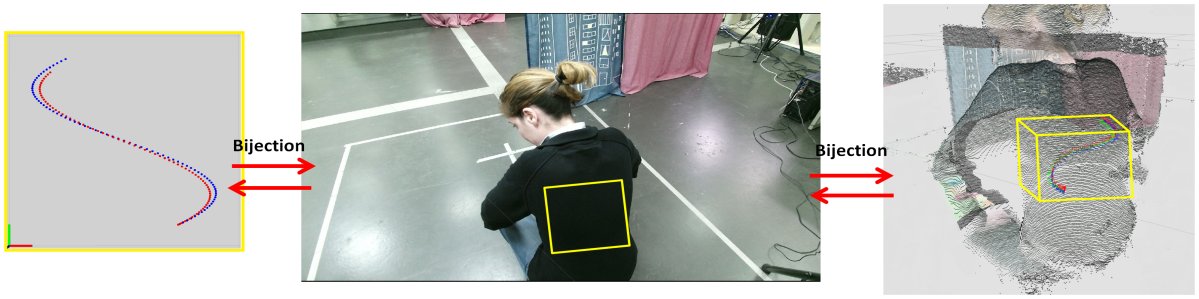


(a) Canonical Space (b) Image Space (c) Task Space

Fig. 2: Three different spaces described in the proposed methodology. (a) 2D space normalized in x,y dimensions notated as "Canonical" space. The sinusoidal path from the Canonical space is transformed the rectangular area on the Image space, using scaling and rotation. (b) 2D Image space is the actual image (of size 512 x 424 pixels) obtained from Kinect sensor. The yellow rectangular area marks the user's back region, as a result of a segmentation algorithm. The transformed path is fitted on the surface of a female subject's back region, using the camera projection transformation. (c) 3D Task Space is the operational space of the robot. The yellow box represents a Cartesian filter, including the points on which the robot will operate.

## IV. BEHAVIORAL BASED MOTION CONTROLLER

The task is described by a predefined stored washing motion $\mathbf{q}_d(t)$ (blue path in Fig. 2(a)) described in the "Canonical" space (e.g. composition of time constrained motion primitives designed for rinsing water on the back region). We make use the following controller to satisfy both the time constraints imposed by the health-care specialist or the user needs (e.g. the user prefers a quicker washing action than the predefined) and the spacial constraints imposed by the region of action (e.g. the back of the user) and the obstacle areas from the 3D operating scene. In this section we present the definition and the convergence proof of the behavioral based motion controller.

In more detail, we utilize a navigation function of the form:

$$\varphi(\mathbf{q},t)=\frac{\gamma(\mathbf{q},t)}{\left[\gamma^{\kappa}(\mathbf{q},t)+\beta(\mathbf{q},t)\right]^{1/\kappa}} \tag{1}$$

where $\kappa>0$, $\gamma$ is the distance to the 2D time constrained washing motion, and $\beta(\mathbf{q})$ is the product of obstacle functions coming from visual feedback, [22].

We consider convergence of the system to a small ball of radius $r>0$ containing the target.

Before defining the control we need some preliminary definitions. We can define the Hessian of the $\varphi$, as $\nabla^2\varphi(\mathbf{q},t)$. Let $\lambda_{\min}$, $\lambda_{max}$, $\hat{v}_{\lambda_{\min}}$, and $\hat{v}_{\lambda_{\max}}$, be the minimum and the maximum eigenvalues of the Hessian, and the corresponding unit eigenvectors. Then we assume the $R$ region, as described in [23], to identify sets of points that contain measure zero sets whose positive limit sets are saddle points: $R=\{\mathbf{q}|(\lambda_{\min}<0)\wedge(\lambda_{\max}>0)\wedge\left(\left|\hat{v}_{\lambda_{\min}}\cdot\nabla\varphi\right|<r_1\right\}$, where $r_1<\min_{S=\{\mathbf{q}:\|\mathbf{q}-\mathbf{q}_d\|=r\}}(\|\nabla\varphi(S)\|)$. If $\left|\hat{v}_{\lambda_{\min}}\cdot\nabla\varphi\right|=0$. The set $R$ consists of the measure zero set of initial conditions that lead to saddle point. Therefore, $r_1$ can be chosen to be arbitrarily small so the sets defined by $R$ eventually consist of thin sets containing sets of initial conditions that lead to saddle points.

*Proposition 1:* The system $\dot{\mathbf{q}}=\mathbf{u}$, under the control law defined by the vector field $u=-\nabla\varphi_\tau$ converges to the set where $\|\mathbf{q}-\mathbf{q}_d\|<r$, almost everywhere[1]. We can define $\nabla\varphi_\tau$, as:

$$\nabla\varphi_\tau=a+b\cdot\frac{a}{f\left(\|a\|^2,r^2\right)-r^2\cdot g(b)\cdot g\left(\|a\|^2\right)} \tag{2}$$

with $f(c,s)=\begin{cases}c, & c\geq s\\ s, & c<s\end{cases}$, and $g(c)=\frac{c}{1+|c|}$, where $a=\nabla\varphi$, $b=\frac{\partial\varphi}{\partial t}$, and $\varphi$ is the defined navigation function (1).

*Proof:* We form the Lyapunov function $V=\varphi(\mathbf{q},t)$ as described by (1), and we can take it's derivative:

$$\dot{V}=\frac{\partial V}{\partial t}+u\cdot\nabla V=b+u\cdot a \tag{3}$$

After substituting the control law $u=-\nabla\varphi_\tau$ by using (2), and since we pursue convergence in the set $\|\mathbf{q}-\mathbf{q}_d\|<r$, we get:

$$\dot{V}=-\|a\|^2+b\cdot\left(1-\frac{\|a\|^2}{\|a\|^2-r^2\cdot g(b)\cdot g\left(\|a\|^2\right)}\right)$$

Therefore, we can discriminate the three cases:

1) $b<0\Rightarrow-1<g(b)<0\Rightarrow$
$\|a\|^2<\|a\|^2-r^2\cdot g(b)\cdot g\left(\|a\|^2\right)<\|a\|^2+r^2\Rightarrow\dot{V}\leq 0$
2) $b>0\Rightarrow 0<g(b)<1\Rightarrow$
$\|a\|^2-r^2<\|a\|^2-r^2\cdot g(b)\cdot g\left(\|a\|^2\right)<\|a\|^2\Rightarrow\dot{V}\leq 0$
3) $b=0\Rightarrow\dot{V}=-\|a\|^2\leq 0$

The sets defined by the set $R$ are by construction repulsive. We make the assumption that the initial conditions of the system are in the set $\{W\}\setminus\mathscr{E}$, where the set $\mathscr{E}=\{\mathbf{q}|\|\nabla V\|<r_1\}$. ■

*Remark 1:* Practically, we have the choice of an $r_1$, such that $r_1<\min\{r_0,\|\nabla V(\mathbf{q}_0,t_0)\|\}$, so we are sure that the system's initial conditions are not in $\mathscr{E}$.

Based on this motion controller the next robot desired pose is extracted and propagated to 3D Task space for execution.

## V. ROBOT REFERENCE BEHAVIOR ADAPTATION USING DEPTH SENSOR DATA

In this proposed approach, we use as input the Point-Cloud data received from the depth sensors, and on-line

[1]i.e. everywhere except a set of initial conditions of measure zero.

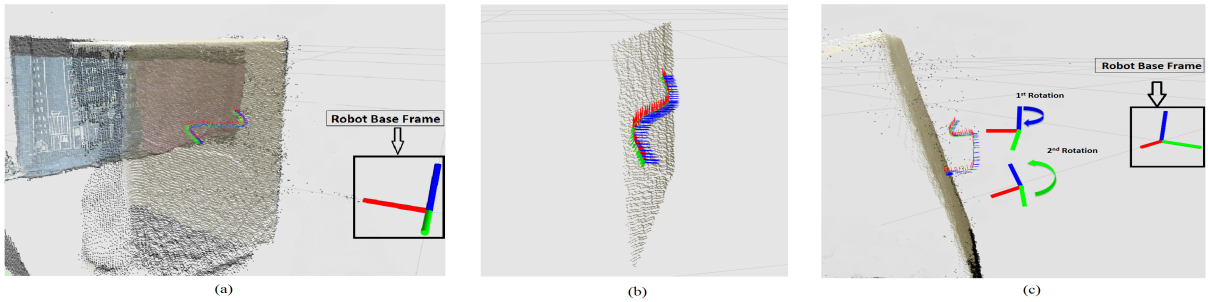


(a) (b) (c)

Fig. 3: Visualization of experimental results with the rectangular box. The blue arrows represent the normal vector to the surface, whereas the green and red arrows represent the tagential axes to the surface. (a) The rectangular box is stationary and the reference path is fitted on its surface. The orientation is calculated w.r.t the robot base frame. (b) A zoomed and segmented version of the box's front side providing a more clear aspect of the path fitted on the surface. (c) The box is rotated initially w.r.t. the z (blue) axis and then w.r.t. the y(green) axis and the calculated path adapts to this motion.

calculate and modify the reference motion, that the robot should execute in order to fulfill a showering task, Fig. 2. In particular, the data from Kinect depth sensors will be processed initially by user perception algorithms, which are currently under development and will be based on Deep Learning techniques [24], providing body parts recognition and segmentation.

The output of these algorithms will be depth images, which will contain depth information only for the pixels that correspond to the body part (denoted as valid pixels) on which the robot will operate (e.g. the back or the legs of the user), Fig. 2 (c). We can define the 2D extends of the body part on the image plane by calculating the minimum and maximum coordinates of the valid pixels along the image axes. The learned motion is followed by the controller and the result is transformed from the 2D "Canonical" space to the image space by performing an anisotropic scaling in order to fit to the projection limits calculated in the previous step, as depicted in up-left side of Fig. 2. Since scaling is a linear transformation we have one-to-one correspondence between the points of the motion on the "Canonical" space and the image space. At each time step one point of the motion is transformed from the "Canonical" space to the image space and then to the task space, i.e. the 3D space that the robot will normally operate, as shown in Fig. 2 (c).

The latter stage of this workflow is implemented by using the depth information from the image space. More specifically, from the depth data of the pixel, which corresponds to the motion point and of its neighboring pixels in the image space, we are able to directly calculate their 3D position. This group of points in the 3D task space form a small planar segment of the body part surface. Computing the mean of this group of points $\mathbf{p}_k \triangleq [p_x^k \quad p_y^k \quad p_z^k]^T$ where $p_x^k, p_y^k, p_z^k$, are the Cartesian coordinates of points $k = 1, ..., n$, and applying eigenvalue decomposition to their covariance matrix, as follows:

$$C = \begin{bmatrix} Cxx & Cxy & Cxz \\ Cyx & Cyy & Cyz \\ Czx & Czy & Czz \end{bmatrix},$$

where

$$C_{ij} = \frac{1}{n}\sum_{k=1}^{n}(p_i^k - m_i)(p_j^k - m_j),$$

and

$$\mathbf{m} = \frac{1}{n}\sum_{k=1}^{n}\mathbf{p}_k \triangleq [m_x \quad m_y \quad m_z]^T$$

with $i, j = \{x, y, z\}$, we are capable of determining the 6D reference pose for the robot. The 3D point, which the robot's end effector should meet, equals to the mean point of the group, whereas the orientation is calculated with the aid of the eigenvectors of the covariance matrix.

The eigenvectors resulting from this decomposition correspond to the principal axis of the 3D data and more specifically, the normal direction of the planar segment is the axis that corresponds to the minimum eigenvalue, i.e. the direction of minimum variance of the data (the blue vector in Fig. 3), and the rest two eigenvectors are defining the tangential plane of the considered region, as depicted with green and red vectors in Fig. 3. Considering these vectors as the reference orientation for the end-effector of the robot, we are able to calculate the angles w.r.t. the robot base frame, which the robotic manipulator should follow. The aim of these calculations is to achieve smoother surface tracking techniques and proper force exertion to the human.

## VI. EXPERIMENTS

### A. Setup Description

In order to test and analyze the performance of the proposed approach, an experimental setup is used that includes a Kinect-v2 Camera providing depth data for the back region of a subject, as shown in Fig. 2 (c) , with accuracy analyzed in [25]. The segmentation of the subjects' back region is implemented, for the purposes of this experiment, by simply applying a Cartesian filter to the Point-Cloud data. The setup also includes a 5 DOF Katana arm by Neuronics, [26] and a HC-SR04 Ultrasonic Range Finder (range $2cm - 400cm$ with accuracy $0.3cm$) for the distance measurements between the robot end-effector and the object or the subject.

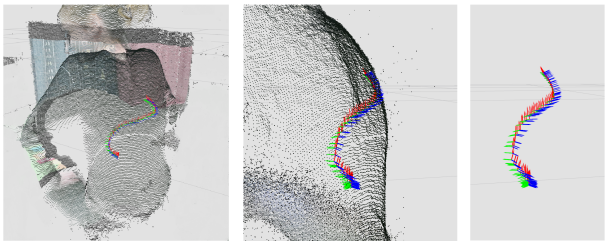


Fig. 4: Experiment on a female subject. (a) Adaptation of the sinusoidal path on the curved surface of a female subject represented with PointCloud data. (b) A zoomed aspect of the experiment depicting in more detail the adaptation of the path. (c) A more clear view of the zoomed path without the PointCloud.

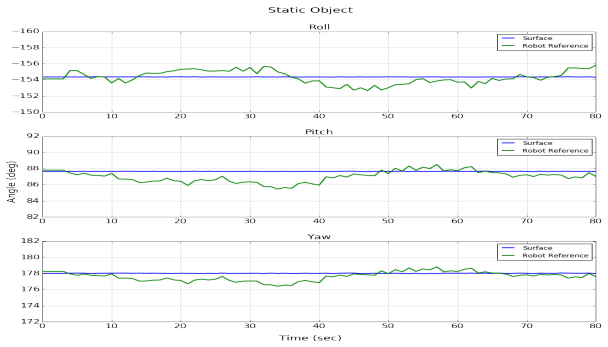


Fig. 5: Evolution of the object's rotations, the reference trajectory orientation and the executed robot end-effector orientations, during the first experiment that involves the static rectangular object.

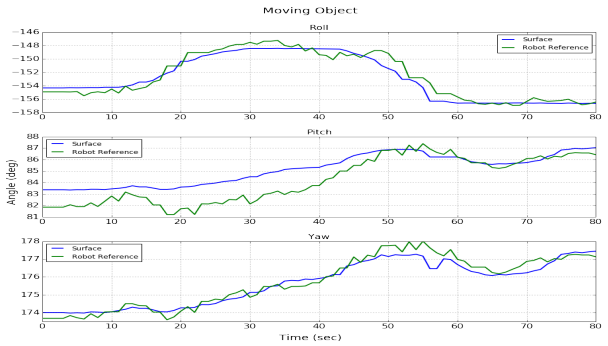


Fig. 6: Evolution of the object's rotations, the reference trajectory orientation and the executed robot end-effector orientations, during the second experiment that involves the moving rectangular object.

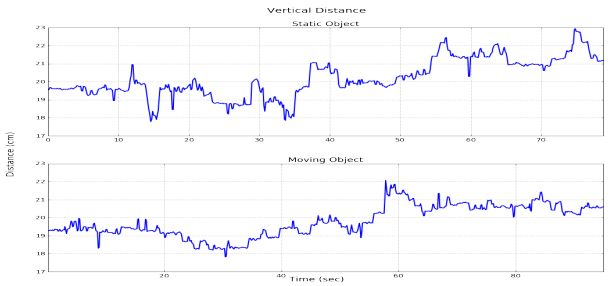


Fig. 7: Perpendicular distance between the Katana end-effector and the experimental subject.

### B. *Validation Strategy and Results*

The experiments conducted include the following of a simple sinusoidal path, keeping simultaneously a constant distance and perpendicular relative orientation to the surface of a rectangular box, that represents a rigid body. Also, the same experiments are conducted on a female subject's back region.

For the **first** and the **second** experiment we employ a rigid and rectangular object for the evaluation of the method (Fig. 3). In particular, we segment the side of the object facing the camera as shown in Fig. 3(b). The reference orientation of this planar segment is calculated with the same procedure described in Section V, using in the calculations the total amount of points constituting the front side of the object. Since the chosen object is non-deformable, the calculated orientation is used as ground-truth. Both the ground-truth orientation and the on-line calculation of the reference pose subject to the same camera accuracy constraints (e.g. errors and noise) analyzed in [25].

During the **first** experiment the box is stationary Fig. 3(a), whereas in the **second** experiment the box performs rotations around y and z axes Fig. 3(c). Furthermore, for evaluation purposes we used an initial set-up including the Katana robot with the described distance sensor, since firstly this approach doesn't take into account the model of the robot and secondly the soft manipulator is currently under construction as shown in Fig. 1. In the **third** experiment, a female is involved (Fig. 4). In this case, there is no ground truth data for total rotation of the subject, since the back region is a non-planar and deformable surface. This experiment was conducted, in order to highlight the adaptability of the algorithm to different users (a female subject with much thinner silhouette than the object).

The blue arrows in Fig. 3 and 4 represent the normal vector to the surface, whereas the green and red arrows represent the tangential axes to the surface. In Fig. 4(a) a general aspect of the experimental scene is shown, whereas in Fig. 4(b)(c) a zoomed and more clear view of the same scene is depicted, showing that the reference path is adapted to the subjects' back region.

In Fig. 5, 6, the evolution of the object's surface rotations w.r.t. the robot base frame and the reference path orientation are depicted. In Table I, the Mean Absolute Error of the object's rotations w.r.t. the reference path orientation are presented in degrees, along with the mean perpendicular distance between the end-effector and the experimental subject. It is obvious, that the calculated reference path manages to compensate with the object's motion, while the under-actuated robotic platform converges to the reference path. The variance of the Mean Absolute Error is primarily affected by the roughness of the object's material.

Moreover, in all experiments the perpendicular distance between the Katana end-effector and the experimental rectangular object is measured with the range-finder sensor and is presented in Fig. 7. Based on these results, the proposed method successfully keeps bounded distance taking into

TABLE I: Mean Absolute Error in Orientation and Mean Distance

| | Roll (deg) | Pitch (deg) | Yaw (deg) | Distance (cm) |
|---|---|---|---|---|
| Static Object | $0.673 \pm 0.443$ | $0.767 \pm 0.553$ | $0.537 \pm 0.408$ | $20.18 \pm 1.055$ |
| Moving Object | $0.721 \pm 0.551$ | $1.01 \pm 0.711$ | $0.284 \pm 0.212$ | $19.79 \pm 0.872$ |

Mean Absolute Error of the calculated reference orientation w.r.t the rotations of the object. The forth column presents the mean and standard deviation of the perpendicular distances between the Katana end-effector and the object.

account the noise inserted by the accuracy of the sensor and the fact that the Katana manipulator is under-actuated for this specific task and during the progress of the motion is stressed to the limits of its dexterous workspace.

The mean time performance of the algorithm presented in Section V over the frames of the experimental procedure is **6ms** (measured with Intel(R) Core(TM) i7-6700K CPU @ 4.00GHz and 16Gb RAM.). The timing performance of the algorithm is low, making the proposed approach computationally efficient for on-line procedures.

## VII. CONCLUSIONS AND FUTURE WORK

This paper presents an efficient algorithm for defining the behavior of a robot's end-effector, whose task is to interact in a friendly way with moving and variably curved body parts. Initially, the complexity of the problem is reduced by using predefined washing paths on a 2D normalized space ("Canonical" space). The washing path is tracked by a navigation function-based controller, which guaranties globally uniformly asymptotic stability. The extracted path points are transformed firstly to the 2D Image space and then to the Task space with two bijective transformations, respectively. In particular, the first bijection includes affine transformations, whereas for the necessary calculations of the second transformation, we have used depth information from a camera and applied eigenvalue decomposition to the covariance matrix of the 3D points around a small region of the body area. The proposed methods are validated through real experiments on a rectangular rigid object and a female subject by using a Kinect camera. The experimental results show, that the calculated reference paths manage to follow the motion and non-planar, deformable surface of the subject's back region.

For further research, we aim to ameliorate this methodology in order to meet any soft robotic manipulation special requirements. Furthermore, we will use paths learned by demonstration of professional carers, in order to make the bathing sequence more human-like. Image processing techniques will also be adopted to increase the method's robustness, to filter the noise of the camera and overcome the occlusions in the image, due to robot motion. Finally, another aspect of the proposed approach is to design the controller directly on the image space, to exploit in a more sophisticated manner the visual feedback information coming from the camera, to achieve for example avoidance of obstacles induced by sensitive areas of the body (e.g. injuries) and to integrate hybrid (force/position) control properties.

## REFERENCES


[1] D. D. Dunlop, S. L. Hughes, and L. M. Manheim, "Disability in activities of daily living: patterns of change and a hierarchy of disability," *American Journal of Public Health*, vol. 87, pp. 378–383, 1997.

[2] S. Katz, A. Ford, R. Moskowitz, B. Jackson, and M. Jaffe, "Studies of illness in the aged: The index of adl: a standardized measure of biological and psychosocial function," *JAMA*, vol. 185, no. 12, pp. 914–919, 1963.

[3] T. Hirose, S. Fujioka, O. Mizuno, and T. Nakamura, "Development of hair-washing robot equipped with scrubbing fingers," in *ICRA, 2012 IEEE*, 2012.

[4] M. Hillman, K. Hagan, S. Hagan, J. Jepson, and R. Orpwood, "The weston wheelchair mounted assistive robot - the design story," *Robotica*, vol. 20, pp. 125–132, 3 2002.

[5] C. Laschi, B. Mazzolai, V. Mattoli, M. Cianchetti, and P. Dario, "Design of a biomimetic robotic octopus arm," *Bioinspiration & Biomimetics*, 2009.

[6] J. Li and J. Xiao, "A general formulation and approach to constrained, continuum manipulation," *Advanced Robotics*, 2015.

[7] J. Li, Z. Teng, and J. Xiao, "Can a continuum manipulator fetch an object in an unknown cluttered space?" *Robotics and Automation Letters*, 2017.

[8] I. D. Walker, "Continuous backbone continuum robot manipulators," *ISRN Robotics*, 2013.

[9] D. B. Camarillo, C. R. Carlson, and J. K. Salisbury, "Task-space control of continuum manipulators with coupled tendon drive," in *Experimental Robotics*. Springer, 2009.

[10] J. Xiao and R. Vatcha, "Real-time adaptive motion planning for a continuum manipulator," in *IROS*. IEEE, 2010.

[11] M. Mahvash and P. E. Dupont, "Stiffness control of a continuum manipulator in contact with a soft environment," in *IROS*. IEEE, 2010.

[12] B. Bardou, P. Zanne, F. Nageotte, and M. De Mathelin, "Control of a multiple sections flexible endoscopic system," in *IROS*. IEEE, 2010.

[13] A. Ataka, P. Qi, A. Shiva, A. Shafti, H. Wurdemann, P. Dasgupta, and K. Althoefer, "Towards safer obstacle avoidance for continuum-style manipulator in dynamic environments," in *2016 IEEE BioRob*, June 2016, pp. 600–605.

[14] A. Ataka, P. Qi, H. Liu, and K. Althoefer, "Real-time planner for multi-segment continuum manipulator in dynamic environments," in *2016 IEEE ICRA*, May 2016, pp. 4080–4085.

[15] H. Liu, X. Deng, H. Zha, and K. Chen, *Real-Time Motion Planning by Sampling Points on Obstacles' Surfaces Towards HRI*. Springer Berlin Heidelberg, 2006.

[16] X. Papageorgiou, H. G. Tanner, S. G. Loizou, and K. J. Kyriakopoulos, "Switching manipulator control for motion on constrained surfaces," *Journal of Intelligent & Robotic Systems*, 2011.

[17] S. Chandra, S. Tsogkas, and I. Kokkinos, "Accurate Human-Limb Segmentation in RGB-D images for Intelligent Mobility Assistance Robots," in *ACVR, ICCV*, Santiago, Chile, 2015.

[18] M. Manti, A. Pratesi, E. Falotico, M. Cianchetti, and C. Laschi, "Soft assistive robot for personal care of elderly people," in *2016 IEEE BioRob*, 2016.

[19] I. Rodomagoulakis, N. Kardaris, V. Pitsikalis, E. Mavroudi, A. Katsamanis, A. Tsiami, and P. Maragos, "Multimodal human action recognition in assistive human-robot interaction," in *IEEE ICASSP*, 2016.

[20] C. Mandery, O. Terlemez, M. Do, N. Vahrenkamp, and T. Asfour, "The kit whole-body human motion database," in *ICAR*, 2015.

[21] Y. Zhou, M. Do, and T. Asfour, "Learning and force adaptation for interactive actions," in *Humanoids*. IEEE, 2016.

[22] E. Rimon and D. Koditschek, "Exact robot navigation using artificial potential functions," *IEEE Transactions on Robotics and Automation*, 1992.

[23] X. Papageorgiou, S. Loizou, and K. Kyriakopoulos, "Motion planning and trajectory tracking on 2-D manifolds embedded in 3-D workspaces," *2005 IEEE ICRA*, 2005.

[24] S.-E. Wei, V. Ramakrishna, T. Kanade, and Y. Sheikh, "Convolutional pose machines," in *IEEE Conference CVPR*, 2016.

[25] L. Yang, L. Zhang, H. Dong, A. Alelaiwi, and A. El Saddik, "Evaluating and improving the depth accuracy of kinect for windows v2," *Sensors Journal*, 2015.

[26] N. AG, "Katana user manual and technical description."